



A TEM study of the incommensurate modulated structure in $\text{Sr}_2\text{CuO}_{3+\delta}$ superconductor synthesized under high pressure

A. Evolution of the incommensurate modulated structure and the electronic structure with post-heat treatment

Y.Y. Wang^{a,*}, H. Zhang^a, V.P. Dravid^a, L.D. Marks^a, P.D. Han^b, D.A. Payne^b

^a Department of Materials Science and Engineering, Science and Technology Center for Superconductivity, Northwestern University, Evanston, IL 60208, USA

^b Department of Materials Science and Engineering, Science and Technology Center for Superconductivity, and Materials Research Laboratory, University of Illinois at Urbana-Champaign, Urbana, IL 61801, USA

Received 13 March 1995; revised manuscript received 20 September 1995

Abstract

Transmission electron imaging, diffraction and spectroscopy techniques are utilized to study the changes in modulated structure and aspects of electronic structure of the high oxygen pressure synthesized superconductor: $\text{Sr}_2\text{CuO}_{3+\delta}$. The presence of an incommensurate modulated superstructure in $\text{Sr}_2\text{CuO}_{3+\delta}$ and its dependence on post-annealing treatment is documented. Transmission EELS indicates that there is a high density of states near the Fermi surface for the modulated phase in as-made ($T_c = 70$ K) and optimally treated ($T_c = 94$ K) specimens, while there is a low density of states near the Fermi surface for over-treated samples with $T_c = 0$ K.

1. Introduction

Hiroi et al. have recently reported the occurrence of superconductivity at a transition temperature of ~ 70 K in $\text{Sr}_2\text{CuO}_{3+\delta}$ [1]. They suggested a tetragonal K_2NiF_4 type structure as the basic structure for this material. In addition, they also reported a superstructure with lattice constants of $4\sqrt{2} a_p \times 4\sqrt{2} a_p \times c_p$. Based on the oxygen nonstoichiometry, Hiroi et al. [1] suggested that half of the apical oxygen is

missing in $\text{Sr}_2\text{CuO}_{3+\delta}$. However, contrary to this model, recent neutron diffraction studies on this compound by Shimakawa et al. [2] indicate that the apical oxygen is fully occupied, whereas the oxygen in CuO_2 plane is half occupied. If oxygen does not fully occupy the vital conducting CuO_2 planes, it raises doubts about our current understanding of superconductivity in the cuprates, which relies on full oxygen occupancy for the CuO_2 planes. On the other hand, there is a possibility that this major phase is not the real superconducting phase and that some other second phase may be responsible for the T_c and the Meissner fraction (which is often less than 15%) observed in this material.

* Corresponding author. Fax: +1-708-491-7820.

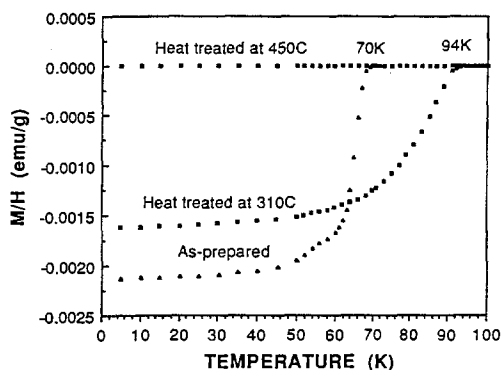


Fig. 1. Diamagnetic susceptibility as a function of temperature for the as-made sample, optimum heat treated sample, and over heat treated $\text{Sr}_2\text{CuO}_{3+\delta}$.

Recently, Han et al. synthesized the high pressure form of $\text{Sr}_2\text{CuO}_{3+\delta}$, and have observed a dependence of T_c on post annealing treatment of the as-prepared material [3]. They noticed that heating the sample to 300°C increased the T_c from 70 to 94 K and that further heating to 450°C caused the sample to lose superconductivity. Fig. 1 shows how the different heat treatments affect T_c for this compound. X-ray diffraction data showed that the basic structure of the material does not change with the different heat treatments.

To investigate the structural and microchemical details of $\text{Sr}_2\text{CuO}_{3+\delta}$, transmission electron diffraction, high resolution electron microscopy and electron energy loss spectroscopy are employed. In Part A of this paper, we report how the crystallography and electronic structure of this phase change with different heat treatments. In part B [12], we detail a structural model to describe the superstructure observed in this compound, based on high resolution electron microscopy imaging and image simulations.

2. Experimental

Superconducting $\text{Sr}_2\text{CuO}_{3+\delta}$ was prepared by a high pressure synthesis method discussed in Ref. [3]. The transition temperature for the as-made sample was 70 K with $\sim 15\%$ Meissner volume fraction at 5 K and 10 Oe. After heat treatment at 310°C in N_2 for 60 min, the T_c increased to 94 K with 11% Meissner volume fraction at 5 K. The sample be-

came non-superconducting after heat treatment at 450°C . In this paper, we will refer to samples of different heat treatments by their T_c : $T_c = 70$ K for the as-made sample; $T_c = 94$ K for the optimally treated sample; and $T_c = 0$ K for the over treated sample.

TEM samples were prepared by polishing the bulk specimen to about $10\ \mu\text{m}$ and subsequently ion beam thinning to electron transparency at liquid nitrogen temperature to minimize ion beam damage. Electron energy loss spectroscopy and electron diffraction measurements were conducted using a cold field emission gun Hitachi HF-2000 microscope, equipped with a Gatan parallel EELS detector. The energy resolution of the zero loss peak was ~ 0.5 eV. Electron energy loss spectra were collected in regions containing the modulated superstructure as shown by electron diffraction patterns. Some minor phases were also discovered in our sample. (Because the main purpose of this paper is to study the phase which was proposed as the superconductor by Hiroi et al., we will not discuss these minor phases further.) It should be noted, however, that no known superconducting phases could be identified within the limit of TEM statistics.

3. Results

3.1. High resolution imaging and the basic structure

The basic structure of as-made, optimum treated, and over treated samples appeared to be quite similar based on high resolution images and electron diffraction patterns. Overall, the principal diffraction spots were the same for all three samples with different heat treatments. However, subtle changes in the HREM images and diffraction patterns were noted. A slight difference in the modulated structure (i.e. different modulation wavelengths) for different heat treatments was observed, which will be discussed in the following sections. Part B of this paper will discuss a detailed analysis of HREM images which allows the modulation structure to be extracted.

3.2. Modulated superstructure

Electron diffraction and microchemical analysis indicated that the major phase in the sample was the

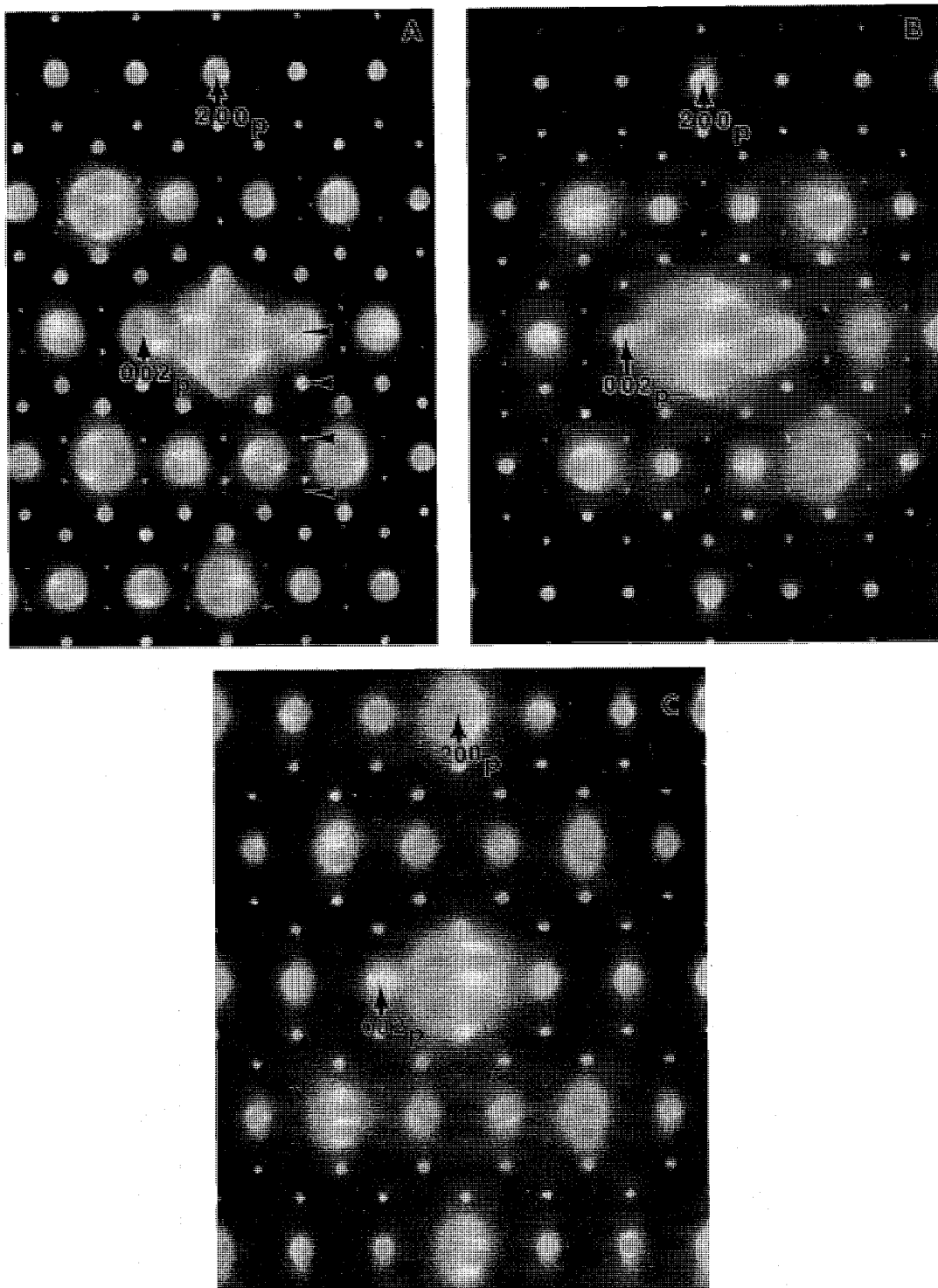


Fig. 2. Diffraction patterns along the $[100]_p$ direction for different heat treatments, (A): as-made sample; (B): optimum treated sample; (C): over treated sample.

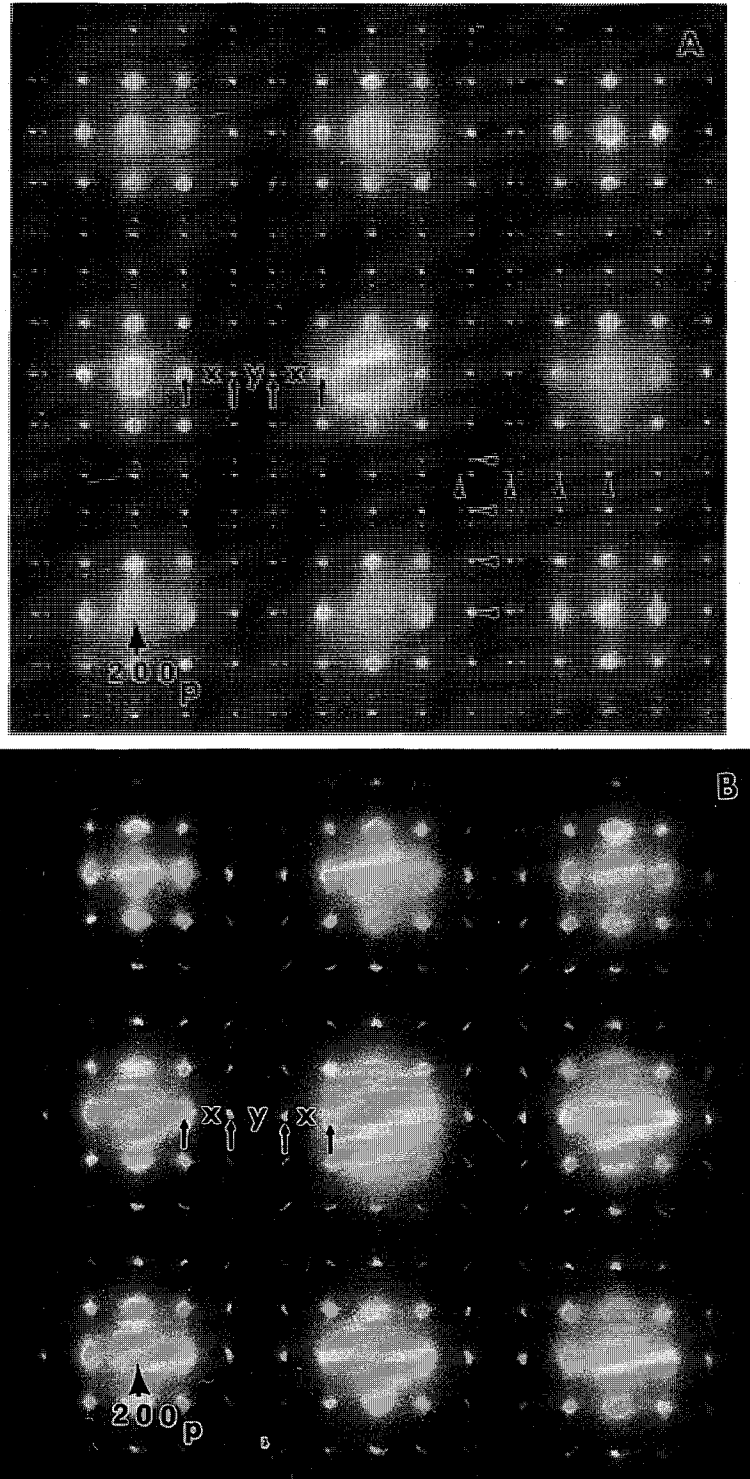


Fig. 3. Diffraction patterns for different heat treated $\text{Sr}_2\text{CuO}_{3+\delta}$ sample, along the $[001]_p$ direction. (A): the as-made sample, in which $y < x$; (B): the optimum heat treated sample, in which $y > x$; (C): the over treated sample, in which $y < x$. In addition, satellite spots near the superstructure spots can be seen in the over treated sample along the $[110]_p$ direction.

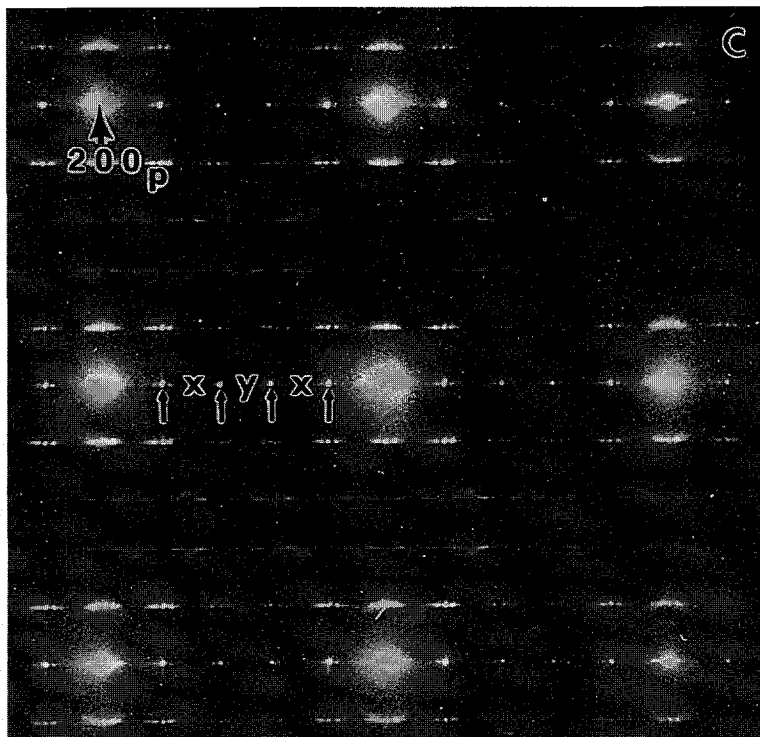


Fig. 3 (continued).

$\text{Sr}_2\text{CuO}_{3+\delta}$ phase with a modulated superstructure. As mentioned earlier, a superstructure was reported by Hiroi et al. [1] and also by Adachi et al. [4]. Hiroi et al. [1] observed a $4\sqrt{2} \times 4\sqrt{2} a_p$ superstructure in their materials; while Adachi et al. observed $5/\sqrt{2} \times 5/\sqrt{2} a_p$ superstructure. In our case, we noticed an incommensurate modulation with an approximate superstructure of $5\sqrt{2} \times 5\sqrt{2} a_p$. The exact wavelength changed with the heat treatment. Fig. 2 shows diffraction patterns along $[100]_p$, while Fig. 3 shows diffraction patterns along $[001]_p$ for specimens with $T_c = 70, 94$ and 0 K. Although the wavelength of the superstructure varied subtly from region to region with the same heat treatment, statistical measurements indicated that: 1) the as-made sample had the smallest wavelength; 2) heating the compound to 310°C resulted in an increased wavelength; 3) overheating the sample at $\sim 450^\circ\text{C}$ gave an intermediate wavelength. The mean values of the wavelengths for different heat treatments are plotted in Fig. 4 with the experimental error (standard error of mean).

In addition to the change of wavelengths, there were also changes in the details of the diffraction patterns. For the as-made sample, the incommensurate wavelengths along $[110]_p$ and $[\bar{1}\bar{1}0]_p$ directions are slightly different, indicating that the superstructure has an orthorhombic symmetry. Additional satellite diffraction spots along $[110]_p$ were also found in the over treated sample, which does not show superconductivity. The additional satellite spots appeared in the $[110]_p$ direction, but did not appear along $[\bar{1}\bar{1}0]_p$. In order to make sure that the additional satellite spots in the diffraction pattern along the $[110]_p$ direction in the over-treated sample were not due to second phase(s), we obtained high resolution images for the optimally treated sample ($T_c = 94$ K) and the over treated sample ($T_c = 0$ K), and calculated the power spectra for these two HREM images. As is shown in Fig. 5, the power spectrum of the image for the over treated sample shows the extra satellite spots near the 1st order superstructure spots along the $[110]_p$ direction, whereas the power spec-

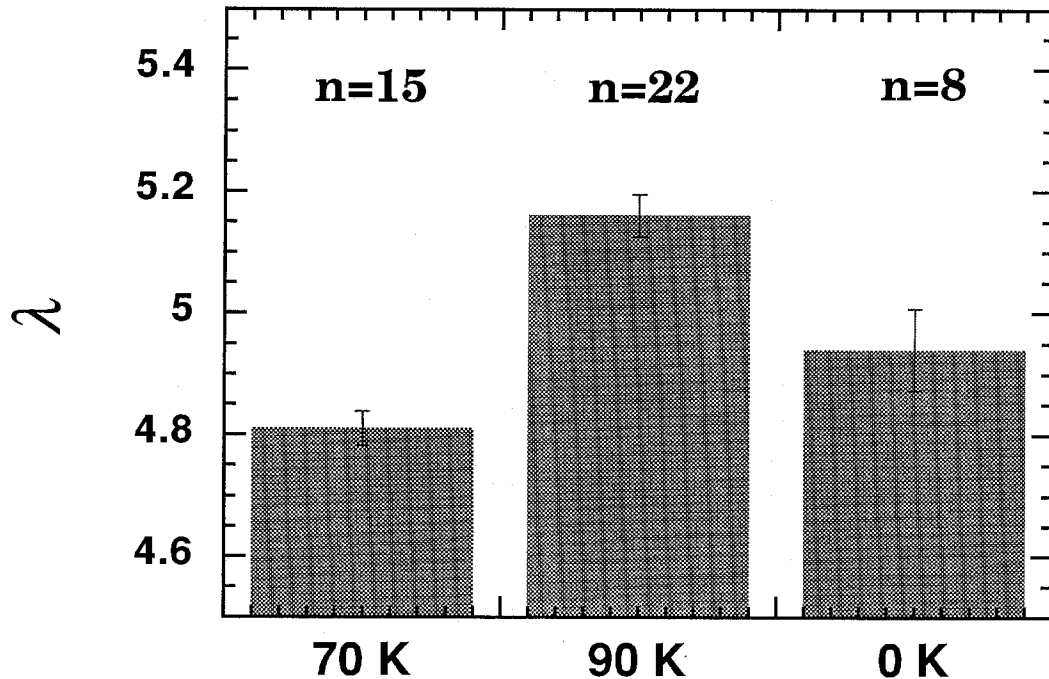


Fig. 4. The mean value of the wavelength of the superstructure for different heat treated samples with experimental error bars, SEM (Standard Error of Mean). The number of the measurement is shown in the figure for the different samples. All the wavelengths shown in the figure should be multiplied by $\sqrt{2}$. Therefore, the wavelength of the incommensurate superstructure is close to $5\sqrt{2}a_p$.

trum of the optimally treated sample does not show the satellite spots. These results conform to the observed electron diffraction patterns in Fig. 3.

3.3. The oxygen K-absorption edge

It is well known for the hole doped cuprate superconductors that the oxygen K-edge fine structure provides valuable information about the charge carriers and their crystallographic confinement [5–7] and that the presence of an O K pre-edge is related to the unoccupied hole states. The density of hole states, to a good approximation, is intimately connected to the oxygen stoichiometry, thus the nature of normal state conductivity in cuprates. Since the strength of the O K pre-edge can be directly related to metallic behavior for cuprates [10,11], it is very interesting to see how the pre-edge changes with different heat treatment of the samples.

Electron energy loss spectra for different heat treatment specimens contain three excitations as shown in Fig. 6. For as-made and optimally treated samples, the first pre-edge excitation is quite clear and sharp; while it is notably weaker for the over treated sample. For comparison, we have also plotted the O K-edge for the “planar defect-free” infinite-layer compound, which is known to be a semiconductor. The Fermi surface for $\text{Sr}_2\text{CuO}_{3+\delta}$ is lowered by ~ 1 eV compared to that for the “defects-free” infinite-layer compound.

4. Discussion

One of the problems in most high pressure synthesized compounds, such as the infinite-layer compound and $\text{Sr}_2\text{CuO}_{3+\delta}$ is whether the major phase is the superconducting phase. The major phase in high

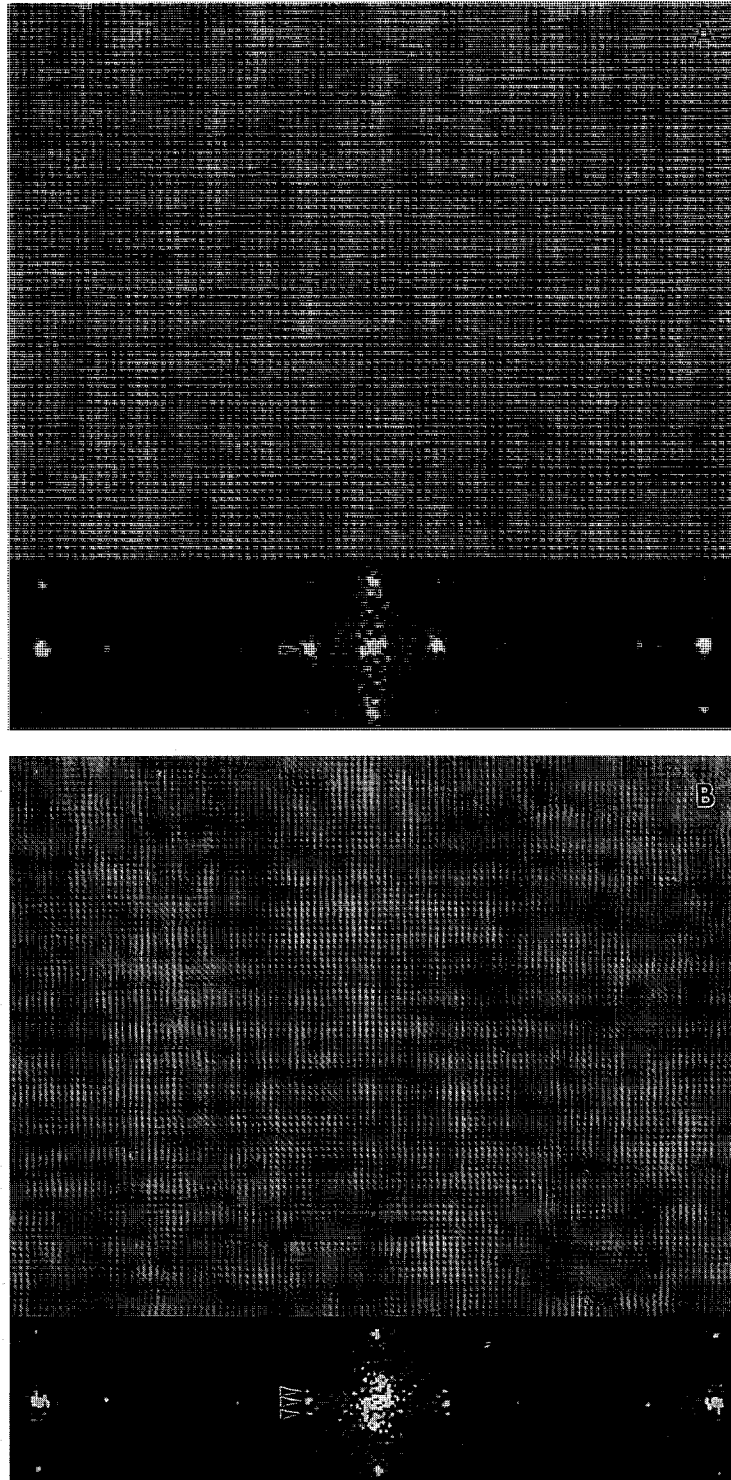


Fig. 5. A) A high resolution image of an optimally treated sample, with a power spectrum at the bottom of the figure. B) A high resolution image of the over-treated sample, with a power spectrum at the bottom of the figure. Notice the satellite spots near the superstructure spot along $[110]_p$ direction in the over-treated sample and their absence in the optimally treated sample.

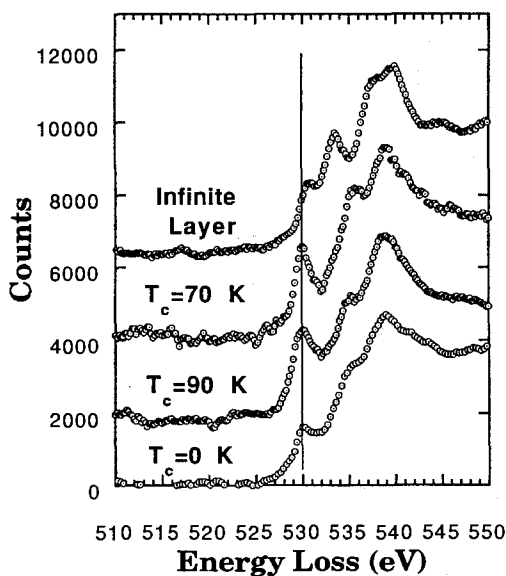


Fig. 6. Electron energy loss spectra of oxygen K-edge for different heat treated samples. The oxygen K-edge for the infinite-layer compound is also shown in the figure for comparison. Notice that for as-made and optimum treated samples, the low Hubbard band is quite clear; whereas for the over treated sample, the intensity of the low Hubbard band is lower. This is consistent with T_c measurements of the samples.

pressure synthesized $\text{Sr}_2\text{CuO}_{3+\delta}$, as reported earlier by Hiroi et al. [1] and by Adachi et al [4] and analyzed in this paper, is the one which contains the modulated superstructure. According to neutron diffraction experiments [2] the oxygen deficiency is located within the CuO_2 planes, contrary to the earlier model [1] where the O deficiency is proposed to be located at the apical oxygen position. If the major phase containing the modulations structure is the superconducting phase, the neutron diffraction data, which suggest oxygen deficient CuO_2 planes in this phase, defy the prevailing understanding that all cuprate superconductors (should) have full oxygen occupancy in the CuO_2 planes. On the other hand, it is also reasonable to doubt whether the superstructure phase is the superconductor phase, because the Meissner fraction of the sample is small ($\sim 15\%$ maximum) and there are minority phases present in the material.

The changes in the modulation wavelength and the O pre-edge fine structure, which coincide with the changes in the superconductor transition tempera-

tures, indicate that there is a correlation between the superconductor transition temperature and the modulated superstructure. It is well known for hole doped superconductor materials that the intensity of the O pre-edge indicates the density of states near the Fermi surface. According to the current understanding of hole doped cuprate superconductor, there are two kinds of electronic states in the normal state, viz. the lower and upper Hubbard band states. In the undoped material, which is not a superconductor, the density of the lower Hubbard state is very small or zero, whereas the density of the upper Hubbard state is high. For example, there is a clear upper Hubbard state in the defect free infinite-layer compound, which is not a superconductor, as shown in Fig. 6 [8,9]. The doping of holes into the CuO_2 plane creates lower Hubbard band, reduces the strength of the upper Hubbard state, and results in charge carriers responsible for the occurrence of superconductivity. However, overdoping suppresses T_c of the sample and results in a normal metallic behavior. This sequence has been observed in $\text{La}_{2-x}\text{Sr}_x\text{CuO}_4$ by both soft X-ray absorption and electron energy loss spectroscopy [10,11].

In $\text{Sr}_2\text{CuO}_{3+\delta}$ the Fermi surface is about 1 eV lower than that of the “defect-free” infinite-layer compound, which is consistent with the energy difference between the upper Hubbard state and the lower Hubbard state [10,11]. In addition, the high density of states near the Fermi surface of the O K-edge for superconductors indicates the presence of charge carrier (holes) and metallic behavior for the material. On the other hand, the low density state at the Fermi surface for the non-superconductor samples indicates low carrier density in the material and suggests semiconductor behavior. Therefore, if they are the superconductor phase, the O K-edge for the superstructure phase is consistent with different T_c 's for different heat treatments.

The change of the superstructure with different heat treatment is also consistent with the change in the lattice constants measured by X-ray diffraction [3]. As reported by Han et al. [3], the superstructure phase has the smallest unit cell volume for the as-made sample, while optimum heat treatment results in an expansion of the principal unit cell without any (significant) oxygen loss. The over treated sample has about 1.87% weight loss and the unit cell

becomes smaller [3]. These results are consistent with the changes of the superstructure wavelength. For the as-made sample, the superstructure has a wavelength smaller than $5\sqrt{2}$ times of the principal lattice constant. For the optimum treated sample the superstructure has a wavelength longer than $5\sqrt{2}$ of the principal lattice constant, and the wavelength of the over treated sample is closer to $5\sqrt{2}$. (The change in length of the principal unit cell is small compared with the change of the superstructure.) As we will show in part B of this paper, the superstructure in this material is due to the cation displacement, resulting in different bond lengths between nearest Cu–Cu ions. According to our model, 50% of the Cu–Cu bond lengths are ~ 4.0 Å and 50% ~ 3.6 Å. In the model, the oxygen atom is located at the longer bond length position, but not at the shorter bond length position. This model suggests half occupancy of oxygen atom in CuO plane and it is consistent with the neutron diffraction experiment, which indicates that the oxygen deficiency is located in the CuO plane. We refer to the CuO plane in this material as the $\text{CuO}_{1+\delta}$ plane. According to the model, the smaller wavelength for the as-made sample indicates more distortion of Cu–Cu bond length. The change of the wavelength in the optimum treated sample indicates a change of bond length between adjacent Cu–Cu ions. This is consistent with the change of the superconducting transition temperature between the as-made sample and the optimum treated sample, because it is well known that the change of the bond length in the CuO_2 plane in other cuprate materials affects the T_c of the sample. The significant weight loss in the over-heated sample is a direct consequence of oxygen loss in the sample. The loss of oxygen causes the material to be underdoped and results in semiconductor behavior. This scenario is consistent with the changes in the oxygen K-edge of the energy loss spectra, as well as the changes in the superstructure for different heat treatments.

5. Conclusion

In this part of the paper, we have shown that different heat treatments of the nominal $\text{Sr}_2\text{CuO}_{3+\delta}$ phase, result in changes in the superstructure pattern

as well as the density of states near the Fermi surface. The change in wavelength of the incommensurate superstructure is consistent with the changes in oxygen distribution in the $\text{CuO}_{1+\delta}$ plane and the superconductor transition temperature of the bulk phase containing $\text{Sr}_2\text{CuO}_{3+\delta}$. The high density of state near the Fermi surface for the superstructure phase for as-made ($T_c = 70$ K) and optimum treated samples ($T_c = 94$ K) indicates metallic behavior of the phase, whereas the low density of state near the Fermi surface in the over treated sample ($T_c = 0$ K) indicates semiconductor behavior of the phase. These results coincide with the different transition temperatures of the superconductor for the post heat treated sample and are consistent with the earlier suggestions that the majority superstructure phase is the superconductor phase in the material.

Acknowledgements

This research was supported by the National Science Foundation (DMR 91-20000) through the Science and Technology Center for Superconductivity. We would like to acknowledge the stimulating discussion with J.D. Jorgensen of Argonne National Laboratory and J.P. Zhang of UCSB.

References

- [1] Z. Hiroi, M. Takano, M. Azuma and Y. Takeda, *Nature*, 364 (1993) 315.
- [2] Y. Shimakawa, J.D. Jorgensen, J.F. Mitchell, B.A. Hunter, H. Shaked, D.G. Hinks, R.L. Hitterman, Z. Hiroi and M. Takano, *Physica C* 228 (1994) 73.
- [3] P.D. Han, L. Chang and D.A. Payne, *Physica C* 228 (1994) 129.
- [4] S. Adachi, H. Tamauchi, S. Tanaka, and N. Mori, *Physica C* 212 (1993) 164.
- [5] J. Fink, *Unoccupied Electronic States* (Springer, Berlin, 1992) p. 203.
- [6] Y.Y. Wang, H. Zhang and V.P. Dravid, *Microscopy Res. Techn.* 30 (1995) 209.
- [7] H. Zhang, Y.Y. Wang, V.P. Dravid, B. Dabrowski, K. Zhang, D.G. Hinks and J.D. Jorgensen, *Physica C* 208 (1994) 231.
- [8] E. Pellegrin, N. Nucker, J. Fink, S.L. Molodtsov, A. Gutierrez, E. Navas, O. Strebel, Z. Hu, M. Domke, G. Kaindl, S. Uchida, Y. Nakamura, J. Merkl, M. Klauda, G. Saemann-

- Ischenko, A. Krol, J.L. Peng, Z.Y. Lin and R.L. Greene, *Phys. Rev. B* 40 (1993) 2217.
- [9] Y.Y. Wang, H. Zhang, V.P. Dravid, P.D. Han and D.A. Payne, *Phys. Rev. B* 48 (1993) 9810.
- [10] C.T. Chen, F. Sette, Y. Ma, M.S. Hybersten, E.B. Stechel, W.M.C. Foulkes, M. Schluter, S.-W. Cheong, A.S. Cooper, L.W. Rupp, Jr., Batlogg, Y.L. Soo, Z.H. Ming, A. Krol and Y.H. Kao, *Phys. Rev. Lett.* 66 (1991) 104.
- [11] H. Romberg, M. Alexander, N. Nucker, P. Adelman and J. Fink, *Phys. Rev. B* 42 (1990) 8768.
- [12] H. Zhang, Y.Y. Wang, L.D. Marks, V.P. Dravid, P.D. Han and D.A. Payne, *Physica C* 255 (1995) 257 (following article).